Influence of capillary confinement on the equilibrium shape of vesicles

1999 J. Phys.: Condens. Matter 11 L51

(http://iopscience.iop.org/0953-8984/11/6/002)

J. Phys.: Condens. Matter **11** (1999) L51–L58. Printed in the UK PII: S0953-8984(99)98225-5

LETTER TO THE EDITOR

Influence of capillary confinement on the equilibrium shape of vesicles

Karim Helal, Thierry Biben and Jean-Pierre Hansen†

Laboratoire de Physique‡, École Normale Supérieure de Lyon, 69364 Lyon cedex 07, France

Received 9 October 1998

Abstract. When a vesicle, delimited by a flexible surfactant membrane, is confined to a slit or a cylindrical capillary, its accessible free volume is reduced. It is shown that the corresponding increase in free energy, taken as the sum of curvature elastic energy and of the lowered entropic contribution, leads to a change of the equilibrium shape, and to a significant shift of the prolate to oblate transition observed for an isolated vesicle, when the reduced bending rigidity is sufficiently small.

Simple vesicles are supramolecular aggregates of amphiphilic molecules dissolved in water which form flexible bilayer membranes in order to minimize contact between the hydrocarbon chains of the lipid and water [1, 2]. Their configurations are determined by bending elasticity, as introduced more than twenty years ago in three seminal papers [3, 4, 5]. Transformations between a large variety of different shapes can be induced, e.g. by changing the temperature or the osmotic conditions [6, 7, 8, 9, 10]. However, the effect of confinement, which results in entropic contributions due to hindered translations and rotations, has received much less attention, despite possible biophysical implications. For example, red blood cells must bend in order to pass through capillaries that are narrower than their size. Although this phenomenon is in general induced by the hydrodynamic flow in the capillary, shape transformations should be observed in the absence of hydrodynamic flow due to the entropic contribution. In this letter we show how confinement can influence the spontaneous shape transformations of vesicles, by allowing for the interplay between the equilibrium shape and the excluded volume correlations with the confining walls.

In order to describe vesicle configurations, several models have been introduced [3, 4, 5, 13] and compared [7, 9, 11]. Recent careful experiments [8, 12] have confirmed that vesicle configurations are governed by the curvature energy of the membrane, subject to constraints on the enclosed volume and the total membrane area and seem to indicate that the so-called area difference elasticity model (ADE) [13, 14] is consistent with all available experimental observations. In order to illustrate the competition between entropy reduction due to confinement and the curvature elastic energy, we consider specifically a special case of the ADE model of Svetina and Zeks with a zero nonlocal bending rigidity. This choice has been made for the sake of simplicity, since our objective is to quantify the effect of entropy rather than to describe precisely all the complexity of the physics of a vesicle. More accurate

† Present address: Department of Chemistry, University of Cambridge, Cambridge CB2 1EW, UK.
‡ Unité de Recherche Associée 1325 du CNRS.

0953-8984/99/060051+08$19.50

descriptions of vesicles can be used. In particular, thermal fluctuations are known to change the equilibrium shapes [15], but including these fluctuations would be technically very demanding and would obscure the physical effect we want to investigate. A zero nonlocal bending has the advantage of making the curvature elastic energy scale-invariant, which will render the subsequent discussion even more transparent. The curvature energy is then:

$$U = \frac{1}{2}\kappa \int_A (C_1 + C_2)^2 \mathrm{d}A \tag{1}$$

where the surface integral is over the total area of the vesicle, κ is the bending rigidity, C_1 and C_2 are the two independent curvatures at each point on the surface. In equation (1) we have omitted the gaussian curvature term, which is a topological invariant and is hence irrelevant to the subsequent discussion. The discussion will also be restricted to axisymmetric shapes throughout, and thermal fluctuations around the shape of lowest energy will be ignored in order to focus on the key issue, which is the competition between curvature energy and confinement entropy. Due to scale invariance of the adopted curvature energy, the equilibrium shape of an isolated vesicle depends only on the dimensionless ratio of the volume V enclosed by the membrane over the volume of a sphere of identical area A [6, 7, 10]:

$$v = \sqrt{36\pi}\,\frac{V}{A^{\frac{3}{2}}}. \tag{2}$$

For a given value of v, the equilibrium shape of the vesicle is obtained by minimizing (1). For isolated vesicles, the equilibrium shape is found to change discontinuously from prolate to oblate for $v = 0.651$, the oblate shape being stable in the range $0.591 < v < 0.651$, while the prolate shape is stable above this range [7].

The problem addressed here is the influence of spatial confinement of a single vesicle on its equilibrium shape, when the parameters κ, v and the degree of confinement are varied. We consider the two cases of a vesicle confined to a slit, i.e. in the space between two parallel planes separated by a distance d, or to a cylindrical tube of diameter d. The confining surfaces are assumed to be adequately coated, to prevent vesicle adhesion.

We define a dimensionless confinement parameter $\xi = \sigma/d$ where σ is the diameter of a sphere of same volume V as the vesicle. As ξ increases, the vesicle is more and more confined to a two-dimensional domain (slit) or to a one-dimensional domain (cylinder); the accessible free volume Ω per unit area of the confining planes, or per unit length of the confining cylinder decreases, resulting in a reduction of the entropy $S = k_B \log \Omega$, where k_B is Boltzmann's constant. A convenient normalization of Ω is chosen, which has no bearing on the final results, since only entropy differences will be relevant. For given values of the reduced bending rigidity $\beta\kappa$ (where $\beta = 1/k_B T$), of the reduced volume v and of the confinement parameter ξ, the equilibrium shape of the confined vesicle is found by minimizing the reduced free energy:

$$\beta F = \beta U - S/k_B \tag{3}$$

under the constraint of fixed enclosed volume and total area of the membrane. In practice we made two approximations to render the free energy minimization tractable:

(a) Rather than deriving and solving the exact Euler–Lagrange shape equations from the extremum condition, we have parametrized the axisymmetric prolate and oblate surfaces by simple two-parameter functions relating the z-coordinate along the axis of symmetry to the radial coordinate r in the plane orthogonal to the axis. The parametrizations read:

$$r^*(z^*) = a\sqrt{1 - (z^*)^2}\sqrt{1 + b(z^*)^2} \qquad \text{(prolate)} \tag{4}$$

$$z^*(r^*) = a\sqrt{1 - (r^*)^2}\sqrt{1 + b(r^*)^2} \qquad \text{(oblate)} \tag{5}$$

where $z^* = z/l$, $r^* = r/l$, and l is the maximum half length of the vesicles which is an irrelevant length scale in the minimization procedure; a and b are the dimensionless shape governing parameters which serve as variational parameters in the minimization of the free energy. The parametrizations (4, 5) reduce the problem of calculating the curvature energy U to simple quadratures:

$$U = U(a,b) = 2\pi\kappa \int_0^1 \frac{(1 + (\dot{r}^*)^2 - r^*\ddot{r}^*)^2}{(1 + (\dot{r}^*)^2)^{\frac{5}{2}}} \mathrm{d}z^* \tag{6}$$

for the prolate case ($\dot{r}^* = \frac{\mathrm{d}r^*}{\mathrm{d}z^*}$) and

$$U = U(a,b) = 2\pi\kappa \int_0^1 \frac{(r^*\ddot{z}^* + \dot{z}^* + (\dot{z}^*)^3)^2}{r^*(1 + (\dot{z}^*)^2)^{\frac{5}{2}}} \mathrm{d}r^* \tag{7}$$

for the oblate case ($\dot{z}^* = \frac{\mathrm{d}z^*}{\mathrm{d}r^*}$).

In the absence of confinement, i.e. in the limit $\xi \to 0$, numerical minimization of the curvature energy $U(a,b)$ with respect to a and b, subject to the constraint of fixed v, yields results very close to the explicit solution of the general shape equation [7] as can be seen in figure 1. In particular, the prolate–oblate transition is found to occur at $v = 0.649$, compared to the 'exact' value $v = 0.651$. Use of the parametrized form of the surface greatly simplifies the subsequent minimization procedure in the presence of confinement, compared to a full solution of the shape equations, while ensuring excellent accuracy.

(b) For a given value of the confinement parameter ξ, calculation of the free volume requires integrations over nontrivial domains resulting from the condition that for any center-of-mass position and orientation of the vesicle axis, the surface of the latter does not intersect the surface of the slit or the cylinder. It must be noted first that in a cylinder or a slit, we can replace the concave shape of the vesicle by its convex envelope without introducing any approximation. This convex envelope can next be approximated by an oblate or prolate spherocylinder as shown in figure 2. A spherocylinder is characterized by two lengths, namely the length L of the cylinder and its diameter D. In the prolate case, the cylinder is capped by two hemispheres of diameter D, and the aspect ratio is $K_p = L/D$; in the oblate case, the cylinder is laterally flanked by the outer half of a torus of major and minor diameters D and L, and the aspect ratio is chosen to be $K_o = D/L$. L and D are chosen such that the 'real' vesicle and the effective spherocylinders have the same volume V and the same maximum length $2l = L + D$ because these are the most relevant parameters governing the excluded volume (refer to the appendix for details of the calculation). The two characteristic lengths L and D of the effective spherocylinders (sc) are then entirely determined by the value of the shape variational parameters a and b in equations (4) and (5) and the reference length l. The corresponding free volume can be calculated analytically for the slit geometry and reduces in the cylindrical geometry to a double integral which is easily calculated numerically (details of the calculation are presented in the appendix). We stress the fact that the effective spherocylinders are only used for the calculation of the free volume and that the 'true' shapes of equations (4) and (5) are used for the calculation of the curvature energy and to impose the constraint on the reduced volume v. Since the effective spherocylinders constitute an approximation for the convex envelope of the actual shape, the ratio $v_{sc} = \sqrt{36\pi}\, V_{sc}/A_{sc}^{(3/2)}$ is not subjected to the constraint $v_{sc} = v$. The total free energy (3) is finally a unique function of the variational parameters a and b, minimized with the constraint $v(a,b) = v$.

The resulting entropies of oblate and prolate effective spherocylinders with aspect ratios K_p and K_o corresponding to the equilibrium shapes of isolated vesicles with $v = 0.65$, are

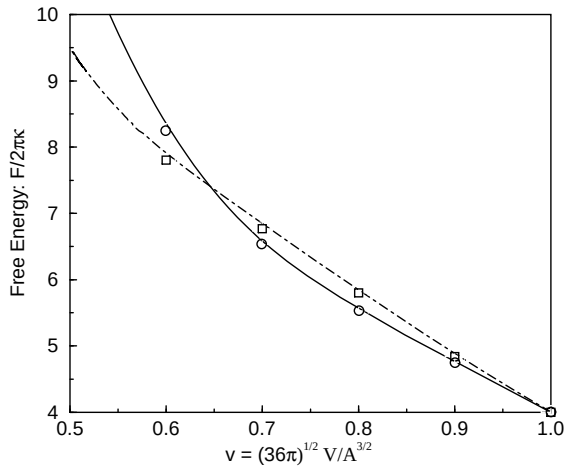

Figure 1. Comparison of the free energies obtained with our parametrization of the vesicle shape with 'exact' results from [7]. The full curve is our result for the prolate shape while the dash-dotted curve is for the oblate shape. Circles and squares are respectively 'exact' results for the prolate and oblate shapes; their size includes our reading uncertainties on the referenced figure.

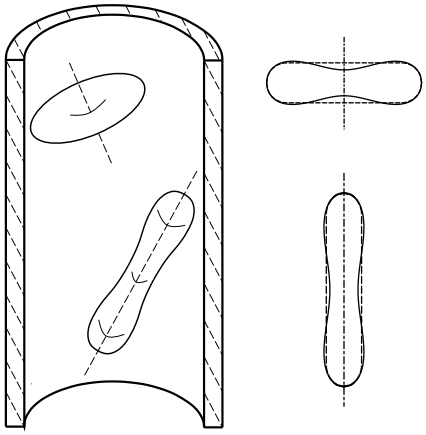

Figure 2. Schematic representation of an oblate and a prolate vesicle in a cylinder. The 'effective' spherocylinders are indicated by dashed lines.

plotted in figure 3 as functions of ξ for slit and cylindrical geometries. In the slit, the entropy of the confined oblate vesicle ($K_o = 2.9$) is always higher than that of the prolate vesicle ($K_p = 3.4$) as one might expect from the 'flatter' topology of the oblate vesicle, and from the fact that the maximum dimension $L + D$ is systematically shorter for the oblate shape. This implies that the effect of confinement will be felt later by oblate vesicles, so that the oblate phase might be expected to be increasingly stabilized with respect to the prolate phase when the confinement parameter increases.

This expectation has been checked by an explicit minimization of the total free energy (3) with respect to the shape parameters a and b, for fixed values of ξ and v. The results for the slit geometry are illustrated in figure 4, where the critical value of v, at which the shape

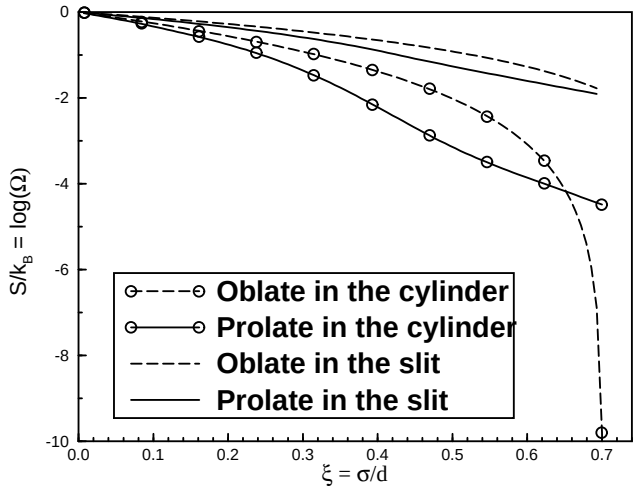

Figure 3. Entropy $S/k_B = \log\Omega$ versus the confinement parameter ξ for oblate ($K_o = 2.9$) and prolate ($K_p = 3.4$) 'effective' spherocylinders in a slit or a cylinder. The break in the full curve corresponds to the situation where the confinement distance d drops below the maximum length of the prolate vesicle.

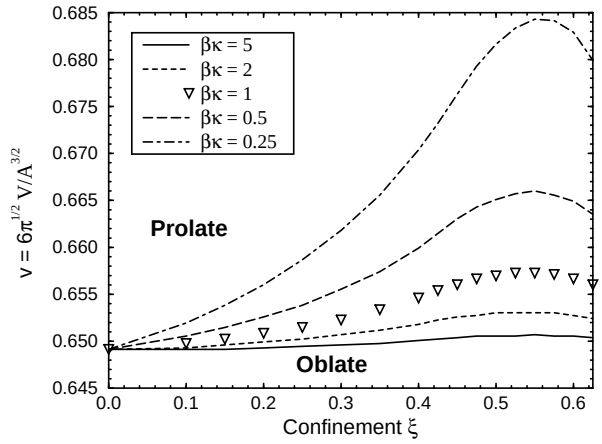

Figure 4. Families of v versus ξ curves at the oblate–prolate transition for several values of $\beta\kappa$; slit geometry.

transformation from prolate to oblate occurs, is plotted as a function of the confinement ξ for several values of the dimensionless bending rigidity $\beta\kappa$. The oblate to prolate transition is shifted to larger values of v as the confinement parameter ξ increases. The effect is more pronounced for the more flexible membranes, characterized by smaller values of $\beta\kappa$, since the weight of the entropic contribution to βF is then larger. The upward shift of v at the transition is relatively modest; even under strong confinement ($\xi = 0.55$) it only amounts to about 1% at $\beta\kappa = 1$.

The effect is more interesting and more significant for a vesicle confined to a cylinder. First, as shown in figure 3, the entropy versus confinement curves associated with oblate and prolate vesicles now cross at $\xi_0 = 0.66$, with the entropy of the prolate phase being larger for

$\xi > \xi_0$. In fact, the free volume associated with the oblate phase vanishes at $\xi_1 = 0.71 > \xi_0$, signalling that an oblate vesicle with the optimum aspect ratio K_o for an isolated vesicle gets 'stuck' in the cylinder. This is reflected in the phase diagram of figure 5 determined by minimizing once more the total free energy (3) of the two shapes for fixed values of v and ξ. For any given value of $\beta\kappa$, the value of v at the prolate–oblate transition first increases with ξ, then goes through a maximum value, before dropping rapidly for $\xi \sim 0.5$. At $\xi = 0.69$, for example, v has dropped by about 7% for $\beta\kappa = 2$, compared to its value for an isolated vesicle.

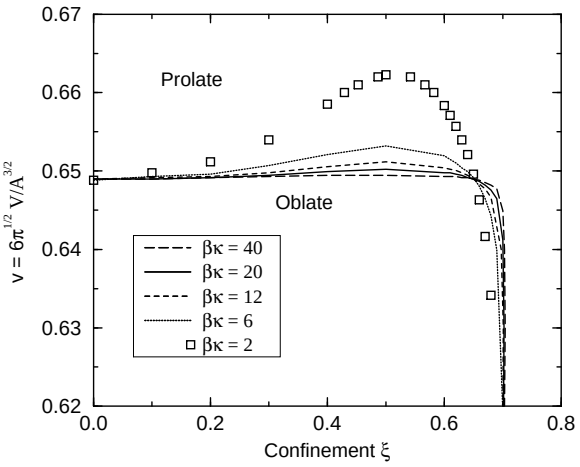

Figure 5. Families of v versus ξ curves at the oblate–prolate transition for several values of $\beta\kappa$; cylindrical geometry.

In the stable (lowest free energy) phase on both sides of the transition, the equilibrium shape of the vesicles is significantly affected by cylindrical confinement, as illustrated in figure 6, which shows the optimum size ratio K_o as a function of ξ for $v = 0.63$ and for a few values of $\beta\kappa$. The values of ξ presented in figure 6 correspond to a situation where the oblate shape is nearly 'stuck' in the cylinder. The stability limit is represented by a square for each value of $\beta\kappa$, which means that above this confinement, the equilibrium shape is prolate. Interestingly, figure 6 shows that the more rigid the membrane is, the more the oblate shape can be affected by the confinement. For $\beta\kappa = 40$, the aspect ratio K_o can be reduced by 8% before this shape becomes unstable. It is important to note that, on the contrary, the prolate shape is not significantly affected by the confinement for $\xi = 0.7$. We must confine the prolate shape to $\xi \simeq 2.1$ to see some effects.

In this simple approach, we completely neglect the thermal fluctuations of the membranes, although we know that they play an important role in the determination of the equilibrium shapes [15]. It is shown in [15] that although the mean shape is strongly affected by fluctuations, the amplitude of the fluctuations around the mean shape is not very large, which means that the excluded volume should not differ much from the excluded volume due to the mean shape. In the present model we have assumed that at least the mean shape could be described by the ADE model, provided we choose an effective value for $\beta\kappa$ and v. It would be of great interest to take into account fluctuations in a confined geometry, although quite difficult in practice, since we can expect the screening of the fluctuations to be an alternative mechanism to induce shape transformations.

The present theoretical formulation lends itself to systematic extensions to allow for

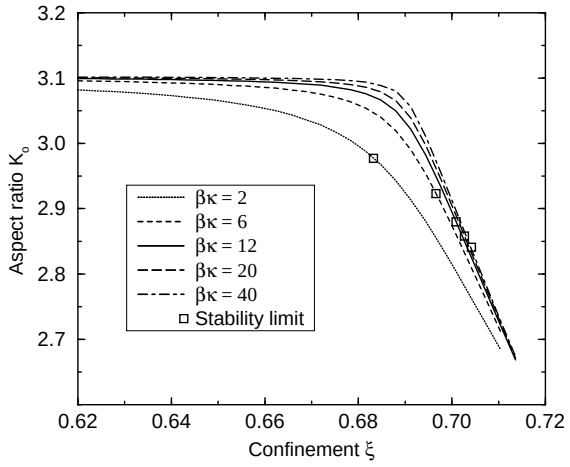

Figure 6. Families of optimum K_o values versus ξ curves in a cylindrical geometry, for $v = 0.63$ and for several values of $\beta\kappa$. The limiting values above which the oblate shapes becomes unstable relatively to the prolate shapes are indicated by the squares.

nonaxisymmetric shapes (which would be clearly relevant for oblate vesicles in a cylindrical capillary) and for nonvanishing nonlocal bending rigidity. Work along these lines is in progress, as well as the exploration of lower values of v where the stomatocyte phase is stable for isolated vesicles.

The authors are indebted to Brian B Rudkin for guiding them towards some important biophysical references.

Appendix

We determine the two characteristic lengths L and D of the effective spherocylinder such that the 'real' vesicle and the effective spherocylinder have the same volume and the same maximum length. With this choice, $L^* = L/l$ and $D^* = D/l$ are the solutions of two equations. Firstly,

$$L^* + D^* = 2 \tag{A.1}$$

and secondly

$$\frac{\pi(D^*)^3}{6} + \frac{\pi(D^*)^2 L^*}{4} = V(a,b) = \frac{4\pi}{3}a^2\left(1 + \frac{b}{5}\right) \tag{A.2}$$

in the prolate case, or

$$\frac{\pi(L^*)^3}{6} + \frac{\pi^2(L^*)^2 D^*}{8} + \frac{\pi L^*(D^*)^2}{4} = V(a,b) = 4\pi a \int_0^1 r^*\sqrt{1-(r^*)^2}\sqrt{1+b(r^*)^2}\,\mathrm{d}r^* \tag{A.3}$$

in the oblate case. Solving these two equations (A.1, A.2) or (A.1, A.3) gives us L^* and D^* as functions of the variational parameters a and b.

The reduced free volume can be calculated analytically for the slit geometry and is equal to

$$\Omega = \pi\left\{\frac{\gamma K}{K+1} + 2(1-\gamma)\right\} \tag{A.4}$$

if $\gamma \leqslant 1$ and

$$\Omega = \pi \left\{ \frac{(K+1-\gamma)^2}{K(K+1)\gamma} \right\} \tag{A.5}$$

if $\gamma \geqslant 1$. $K = (L/D)^{\pm 1} = (L^*/D^*)^{\pm 1}$ is, respectively, the aspect ratio of the prolate and oblate spherocylinders. γ is equal to

$$\gamma_{\text{prolate}} = \frac{(K+1)\xi}{\left(1+\frac{3}{2}K\right)^{\frac{1}{3}}} \tag{A.6}$$

in the prolate case, and to

$$\gamma_{\text{oblate}} = \frac{(K+1)\xi}{\left(1+\frac{3}{4}\pi K+\frac{3}{2}K^2\right)^{\frac{1}{3}}} \tag{A.7}$$

in the oblate case. ξ is the confinement parameter.

In the cylindrical geometry, the reduced free volume reduces to a double integral which is easily calculated numerically. For the prolate case we have

$$\Omega = \left\{ 1 - \frac{\xi}{\left(1+\frac{3}{2}K\right)^{\frac{1}{3}}} \right\}^2 \left\{ 2\pi - 8\int_{\alpha_0}^{1} \alpha \mathrm{d}\alpha \int_{\frac{1-\alpha}{\beta}}^{1} \frac{\min\left(\arccos\left(\frac{1-\alpha^2-\beta^2x^2}{2\alpha\beta x}\right), \frac{\pi}{2}\right)}{\sqrt{1-x^2}} x \mathrm{d}x \right\} \tag{A.8}$$

where $\alpha_0 = \max(1-\beta, 0)$ and $\beta = \xi K / \left((1+\frac{3}{2}K)^{\frac{1}{3}} - \xi \right)$.

For the oblate case, however, the expression is complicated and lengthy, and we do not reproduce it here.

The entropy contribution to the free energy is then an explicit function of the two characteristic parameters L^* and D^* of the spherocylinders and of the confinement ξ. Since L^* and D^* are themselves uniquely determined by the variational parameters a and b, the total free energy is a unique function of the variational parameters a and b which we minimize with the constraint of fixed reduced volume $v(a, b) = v$ and for given values of the confinement ξ and of the reduced bending rigidity $\beta\kappa$.

References

[1] Lipowsky R 1991 *Nature* **349** 475–81
[2] Andelman D 1989 *Statistical Mechanics of Membranes and Surfaces* ed D Nelson, T Piran and S Weinberg (Singapore: World Scientific)
[3] Canham P B 1970 *J. Theoret. Biol.* **26** 61–81
[4] Helfrich W 1973 *Z. Naturf.* **28c** 693–703
[5] Evans E 1974 *Biophys. J.* **14** 923–31
[6] David F and Leibler S 1991 *J. Physique* **1** 959
[7] Seifert U, Berndl K and Lipowsky R 1991 *Phys. Rev. A* **44** 1182–1202
[8] Berndl K, Käs J, Lipowsky R, Sackmann E and Seifert U 1990 *Europhys. Lett.* **13** 659–64; Käs J and Sackmann E 1991 *Biophys. J.* **60** 825
[9] Miao L, Seifert U, Wortis M and Döbereiner H G 1994 *Phys. Rev. E* **49** 5389–407
[10] Peliti L 1996 *Fluctuating Geometries in Statistical Mechanics and Field Theory* (Les Houches, Session LXII) ed F David, P Ginsparg and J Zinn-Justin (Amsterdam: North-Holland)
[11] Seifert U 1997 *Adv. Phys.* **46** 13–137
[12] Döbereiner H G, Evans E, Kraus M, Seifert U and Wortis M 1997 *Phys. Rev. E* **55** 4458
[13] Svetina S and Zeks B 1989 *Eur. Biophys. J.* **17** 101–11
[14] Heinrich W, Svetina S and Zeks B 1993 *Phys. Rev.* E **48** 3112–23
[15] Heinrich V, Sevsek F, Svetina S and Zeks B 1997 *Phys. Rev.* E **55** 1809